Dental Materials Journal 2020; 39(5): 877–882

Development of a novel bioactive titanium membrane with alkali treatment for bone regeneration

Hanako UMEHARA, Kazuya DOI, Yoshifumi OKI, Reiko KOBATAKE, Yusuke MAKIHARA, Takayasu KUBO and Kazuhiro TSUGA

Department of Advanced Prosthodontics, Hiroshima University Graduate School of Biomedical Sciences, 1-2-3, Kasumi, Minami-ku, Hiroshima 734-8553, Japan
Corresponding author, Kazuya DOI; E-mail: kazuya17@hiroshima-u.ac.jp

This study evaluates a bioactive titanium membrane with alkali treatment for stimulating apatite formation and promoting bone regeneration. The titanium thin membranes were either treated with NaOH (alkali-group) or untreated (control). Each sample were incubated in simulated body fluid. Subsequently, the composition of the surface calcium deposition, its weight increase ratio, and optical absorbance were evaluated. Then, the bone defect was trephined on the rats calvaria and covered with each sample membrane or no membrane, and the bone tissue area ratio (BTA) and bone membrane contact ratio (BMC) were evaluated. The spherical crystalline precipitates formed in both groups. In the alkali-group after 21 days, the precipitates matured, forming apatite-like precipitates. The alkali-group showed higher Ca and P contents and weight increase ratios than the control. The alkali-group exhibited a higher BMC than the control in the central area. Thus, this novel membrane has high apatite-forming and bone regeneration abilities.

Keywords: Titanium membrane, Guided bone regeneration, Alkali treatment

INTRODUCTION

Titanium membranes are used as a barrier membrane for guided bone regeneration (GBR) because of their superior biocompatibility and mechanical strength[1-3]. Titanium is a bioinert material, and as such, it does not have a bioactive ability to accelerate bone formation[4,5]. Therefore, various modification methods including grit blasting, acid etching, titanium plasma spraying, and other methods have been applied to modify titanium parts such as implant bodies[6-12]. Among these modification methods, chemical methods such as acid etching or alkali treatment are often used because of their simplicity[6-14]. A titanium surface modified by a strong acid or alkali solution can form an apatite layer when immersed in simulated body fluid (SBF)[13-15]. This layer is expected to create a bioactive surface on thin titanium membranes, which would be beneficial for GBR. An alkali hydrothermal surface treatment was reported to enhance bone integration of titanium implants[16]. However, reports have been limited to assessing solid titanium structures such as disks or implant bodies. In addition, chemical treatment methods cause problematic corrosion on the titanium structure. In fact, our previous study demonstrated that an acid treatment significantly decreased the mechanical strength of a thin titanium membrane[17]. Meanwhile, alkali treatment is one of the most extensively investigated methods for modifying titanium surfaces, and its efficiency has been confirmed by many reports[18-20]. An alkali treatment created a TiO_2 layer on the thin titanium membrane surface, which in turn led to a superhydrophilic nanoporous structure on the surface without affecting the mechanical strength[17]. The surface of this alkali-treated titanium membrane is expected to enhance bone formation, however this aspect of titanium membranes has not been evaluated.

The purpose of this study was to evaluate the alkali-treated titanium membrane to stimulate apatite-forming ability upon immersion in SBF and to promote new bone regeneration *in vivo*.

MATERIALS AND METHODS

Sample preparation

Pure titanium thin membranes (20 μm thick, TR270C, Takeuchi kinzoku-hakufun kogyo, Tokyo, Japan) were used in this study. The samples prepared rectangular shape: 10 mm long and 20 mm wide. To wash and treat all over the surface, we folded the membranes in half. The surface treatment process was the same as that in our previous study[17]. For the control group, the membranes were separately washed in an ultrasonic bath with acetone and distilled water for 1 h each and dried overnight in a 37°C oven.

For the alkali groups, membranes were washed the same way as for control group and then soaked in 20 mL/membrane of a 5 N NaOH solution (NACALAI TESQUE, Kyoto, Japan) and incubated at 60°C for 24 h. After incubation, the membranes were washed with distilled water for 1 h and dried in a 37°C oven.

1. Surface structure

The surface structures of each group were observed by scanning electron microscopy (SEM; JMS-7300F, JEOL, Tokyo, Japan). One sample each from these groups were attached to a sample stage with carbon adhesive tape

Color figures can be viewed in the online issue, which is available at J-STAGE.

Received Jul 16, 2019: Accepted Nov 12, 2019
doi:10.4012/dmj.2019-222 JOI JST.JSTAGE/dmj/2019-222

and imaged. All samples were sputter-coated with Pt (JEC-3000FC, JEOL) before observation.

2. Surface roughness
The surface roughness values of each sample group were measured using a contact-type surface roughness measuring device (DSFP900K31, Kosaka Laboratory, Tokyo, Japan). The measurement length was 0.40 mm and cut off value was λc0.08 mm.

Apatite formation in SBF
Hank's balanced salt solution without phenol red (HBSS10-527F, Lonza, Walkersville, MD, USA) was used as SBF, which had an ion concentration nearly equal to that of human body fluid (Na^+=142.0, K^+=5.0, Ca^{2+}=2.5, Mg^{2+}=1.5, Cl^-=147.8, HCO_3^-=4.2, HPO_4^{2-}=1.0, and SO_4^{2-}=0.5 mM). Each sample was soaked at 37°C in 2.5 mL of SBF in a non-treated plastic well plate. The samples were folded at a 90° angle in the center and placed so that the whole was in contact with the SBF.

The solution was changed every day, and the immersion periods were 7, 14 and 21 days. After immersion in SBF for various periods, samples were removed from the solution, gently washed with distilled water, and dried at 37°C in an oven.

1. Observation of precipitate structure
A sample from each group was observed by SEM with a previous described method.

2. Evaluation of surface composition
Samples were fixed on the stage with carbonate adhesive tape. Then, we performed electron probe microanalysis (EPMA-1720H, SHIMADZU, Kyoto, Japan). The conditions were an acceleration voltage of 15 kV, beam current of 100 nA, and beam size of 100 μm.

3. Measurement of weight increase ratio
Samples were weighed using an electronic balance (AUW120D, SHIMADZU) before and after immersion in SBF. From the obtained data, the increase ratio was calculated for each membrane (%=after soaking/before soaking×100, n=5).

4. Measurement of calcification
Samples were immersed in a 24-well plate (0.5 mL/well) containing alizarin red (ARD-A1, PG Research, Tokyo, Japan) and stained for 30 min at room temperature. Then, samples were washed with distilled water in order to stop the staining. The distilled water in the well was removed as much as possible, formic acid were added and allowed calcified nodules to dissolve. The plate was stirred for 10 min, and the dye was eluted. Next, 100 μL of each eluate was transferred to a 96-well plate to measure the optical absorbance at 450 nm (n=5).

Animal experiments
The animal studies were approved by the Research Facilities Committee for Laboratory Animal Science, Hiroshima University School of Medicine (approval number A18-1-00). Twenty-one male Sprague-Dawley rats (8 weeks old, body weights of approximately 250–300 g) were used in this study. All procedures were performed under general anesthesia with isoflurane and sodium pentobarbital (40 mg/kg intraperitoneal, Somnopentyl, Kyoritsu Seiyaku, Tokyo, Japan). After shaving and disinfecting with iodine, the skin and periosteum of the cranial region was cut. The critical-sized bone defect (diameter: 6 mm)[21] was trephined in the center of rat calvaria (Fig. 1a). The defect area was covered with the alkali-treated membrane, control membrane, or no membrane (denoted by the alkali, control, and without-membrane groups, Fig. 1b). Four weeks later, tissue blocks were harvested. The blocks with membranes at the calvaria were dehydrated using ascending concentrations of ethanol and embedded in light-polymerized polyester resin (Technovit 7200VLC, Heraeus Kulzer, Wehrheim, Germany). Photo-polymerization equipment was used (BS5000, EXAKT Apparatebau, Norderstedt, Germany) to ensure complete polymerization, and the specimens were sectioned with a high-precision diamond disk to produce 200-μm-thick cross-sections. Undecalcified specimens were ground to a thickness of approximately 90-μm with a grinding machine (MG5000, EXAKT Apparatebau, Chemnitz, Germany) and stained with toluidine blue. A light microscope was used for histological examination of the specimens. Using ImageJ, the obtained tissue specimen images were examined to determine the bone tissue area ratio (BTA). BTA was defined as new bone tissue area divided by the total defect area (the area surrounding by

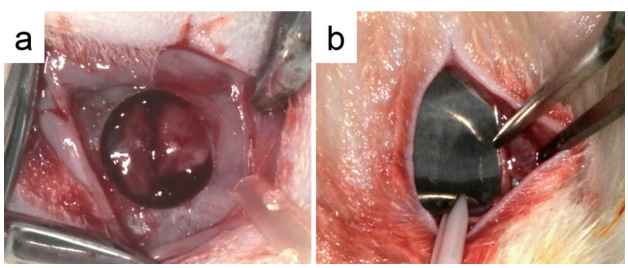

Fig. 1 The critical-sized bone defect was prepared in the center of rat calvaria (a) and covered with a membrane sample (b).

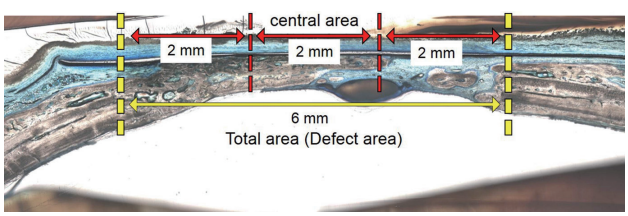

Fig. 2 The BTA and BMC were measured from the total bone defect area and central portion which is middle of one of the three divisions of the defect area.

a line connecting the upper end section and the lower end section of the original defect area). The bone membrane contact ratio (BMC) was calculated as the length of the bone contact portion divided by the entire length of the membrane on the bone defect (n=7).

The BTA and BMC were measured from the overall bone defect region and central portion which is middle of one of the three divisions of the defect area (Fig. 2).

Statistical analyses

All data were analyzed at the 5% significance level using one-way analysis of variance following the Mann-Whitney U test (measurement of the weight increase ratio and BMC) or Fisher's test (measurement of calcification and BTA). Data are expressed as the mean±standard deviation (SD).

RESULTS

Observation of morphology and crystal structure

In the SEM images of samples, the control sample had a rough surface with grooves and indentations (Fig. 3a). The alkali-treated sample had a nano pores structure on the surface (Fig. 3b).

Surface roughness

The Ra values of alkali samples were significantly higher than those of control samples. (Table 1).

After 7 days of immersion in SBF, precipitate layers were observed on the surface of both samples (Figs. 4a, d). Under high magnification, dendritic precipitation was detected in both samples (Figs. 4g, j). However, spherical crystalline apatite structures were not detected. After 14 days, spherical crystalline structures were observed on the dendritic precipitation layer in both groups (Figs. 4b, e). Under high magnification, spherical crystalline apatite structures were clearly detected in both samples (Figs. 4h, k). More crystalline apatite formed in the alkali group than in the control group. After 21 days, large amounts of spherical crystalline apatite structures were detected covering the precipitate layer (Figs. 4c, i). Particularly in the alkali sample, spherical crystalline apatite structures were more mature and larger than those in the control (Figs. 4f, l)

Surface composition

After 7, 14, and 21 days, the Ca and P contents were determined for all alkali and control group samples (Table 2). After 7 days, the alkali group showed higher Ca and P contents than the control group.

Weight increase ratio

The weight increase ratios of the 14 and 21 days alkali samples were significantly higher than those of control samples. There was no difference between the 7 days samples of both groups (Fig. 5).

Calcification assessment

Calcification was significantly higher in all alkali periods of samples than in the controls. However, there were no difference among the alkali samples after different periods of time, nor among the control samples immersed for different times (Fig. 6).

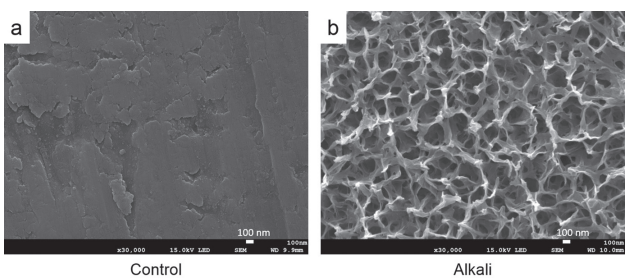

Fig. 3 SEM observations of the surface structure.
(a) control sample, (b) alkali-treated sample. TiO_2 layer of nano scale pores was observed.

Table 1 Surface roughness (Ra)

	μm
control group	0.013 (0.001)
alkali group	0.036 (0.003)**

All values are the mean (SD).
**compared to control group (n=5, p<0.01)

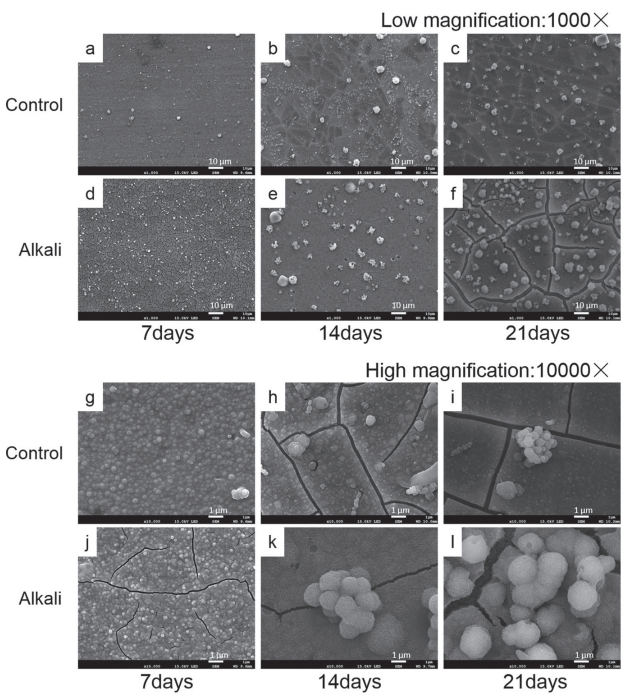

Fig. 4 SEM observations of the surface structures after immersion in SBF.
Control group: low magnification (a, b, c), high magnification (g, h, i). Alkali group: low magnification (d, e, f), high magnification (j, k, l).

Table 2 Surface composition

		Atom (wt%)				
		C	O	Ti	Ca	P
control group	0 day	0.26	5.91	93.8	—	—
	7 days	0.64	35.02	54.27	4.52	4.36
	14 days	0.65	42.78	40.44	7.52	7.09
	21 days	0.44	43.13	32.4	11.01	10.28
alkali group	0 day	2.58	23.65	73.69	0.08	—
	7 days	0.54	42.17	36.13	9.46	8.24
	14 days	0.71	43.94	32.75	10.27	8.83
	21 days	1.41	38.62	38.82	9.37	8.01

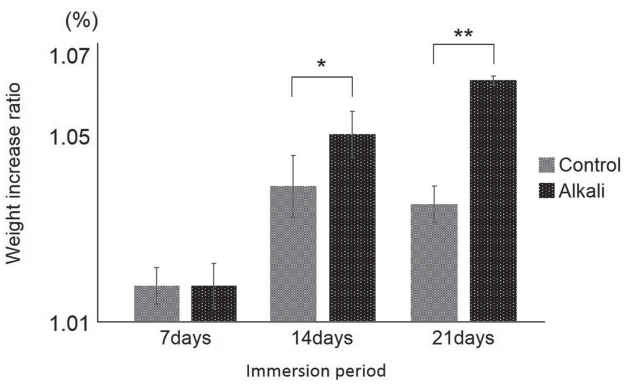

Fig. 5 Weight increase ratio as a function of immersion period (n=5, * p<0.05, ** p<0.01).

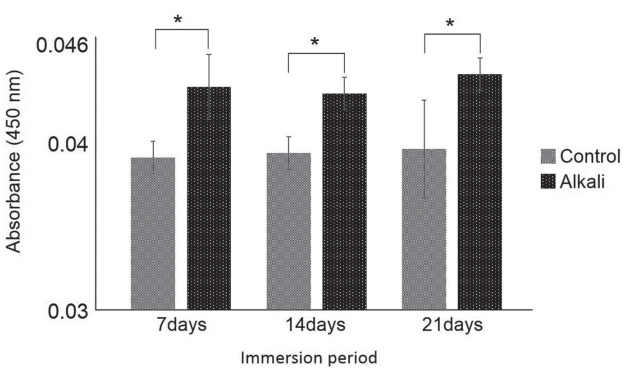

Fig. 6 Optical absorbance due to calcium concentration after immersion in SBF.
Significant differences were detected in each group (n=5, p<0.05).

Histological observations

Newly formed bone was observed in the marginal portion of the alkali (Fig. 7a) and control groups (Fig. 7b). In the central portion, more bone formation was observed beneath the alkali-treated membrane (alkali group) than under the untreated titanium membrane (control group). In contrast, the without-membrane group exhibited insufficient newly formed bone (Fig. 7c).

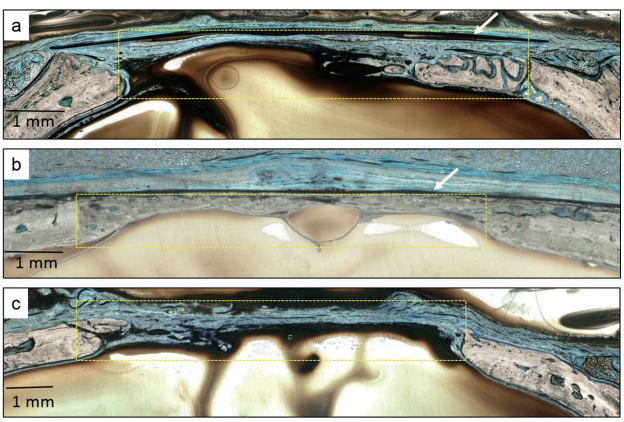

Fig. 7 Histological observations.
The yellow dashed rectangles indicate the bone defects. The arrows indicate the membrane. (a) control group, (b) alkali group, (c) without-membrane group.

Histomorphometrical examination

The BTA of the alkali and control groups were significantly higher than that of the without-membrane group, in both the total defect area and the central bone area. In the central area, the alkali group showed a significantly higher BTA than the without-membrane group, and there was no difference between the control and without-membrane groups. Over the total defect area, there was no difference between the BMC of the control and the alkali groups. On the other hand, the alkali group showed a significantly higher BMC in the central area than control group (Table 3).

DISCUSSION

Surface topographies such as roughness or charge affect osteoconduction and osseointegration[22]. In this study, we selected an alkali treatment using NaOH solution to modify titanium membranes. According to the SEM

Table 3 Measuremns of BTA and BMC

	BTA (%)		BMC (%)	
	total area	central area	total area	central area
Control group	35.1 (20.6)*	21.4 (21.4)*	21.6 (12.1)	8.0 (13.7)
Alkali group	37.9 (13.0)*	33.1 (17.1)**	42.5 (28.8)	41.1 (29.3)*
Without membrane	11.7 (4.6)	1.5±2.6		

All values are the mean (SD).
*compared to without membrane (p<0.05)
**compared to without membrane (p<0.01)
(n=7)

All values are the mean (SD).
*compared to control (p<0.05)
(n=7)

images, the alkali treatment creates a nanoporous network structure on the titanium surface. In our previous study, an alkali-treated titanium membrane showed a modified surface with a superhydrophilic and uniform nanoporous structure similar to that of solid titanium[17]. In this study, we evaluated apatite like crystal precipitation after immersion in SBF. This method is a recognized technique for evaluating whether a biomaterial has bioactive properties and mimics actual *in vivo* behavior. This TiO_2 layer is important to the mechanism of apatite formation in SBF because when it is immersed in SBF, an apatite layer forms on the surface[13,14].

The apatite forms *via* the following process: Na^+ ions on the titanium surface are exchanged with H_3O^+ ions in SBF, and Na^+ ions released. As a result, Ti–OH groups are created on the surface, which are essential for apatite nucleation. As the pH increases, negatively charged Ti–OH groups preferentially combine with the positively charged Ca^{2+} ions in SBF. This process accelerates the crystalline reaction of apatite[23,24]. According to the SEM observations of samples immersed in the SBF, alkali samples after 14 and 21 days clearly showed spherical crystalline apatite-like structures. The weight increase ratios of the alkali samples after 14 and 21 days were significantly higher than those of the control sample. The aspect is considered that difference in the weight change due to the weight of the calcium phosphate composite deposited on the surface in SBF. In the SEM images of the samples immersed for 7 days, each sample exhibits a deposited calcium phosphate composite. There was no significant difference in the weight increase ratio because of the slow rate of crystal growth. Alizarin red S stains deposited calcium; thus, it is used in colorimetric testing of calcification. The optical absorbance results of the alkali samples were significantly higher than those of the control samples, in agreement with the weight increase ratio results. These results suggest that more calcium phosphate deposited on the titanium surface of the alkali-treated samples than on the control samples. However, there is no difference between immersion periods in SBF among each group. These results suggest that alizarin staining reflects the calcium concentration, but it does not reveal information on the crystallinity. Thus, the calcium induced Ti–OH surface, which changed the topography of charged and surface area. The EPMA results also support that Ca and P were derived from calcium phosphate deposition, and crystal growth in the alkali group was faster than that of control during the first 7 days period. Our findings on the ability of alkali-treated thin titanium membranes to form apatite-like structures are consistent with those of other studies performed on solid titanium objects. These findings indicate that the crystallization of apatite is stimulated on the surface of alkali-treated titanium membrane.

According to the histological analysis, the control group and alkali group exhibited newly formed bone in the marginal portion. However, not enough new bone formed in the without-membrane group to be detected. This result suggests that the membrane served as a scaffold for bone regeneration from the surrounding parent bone tissue. On the other hand, the central portion of bone tissue was detected in alkali group compared with control group. This area is far from the surrounding bone and seems to exhibit limited osteoconduction. Therefore, the bone formation at central portion is affected by the surface properties of titanium membrane. As mentioned above, a TiO_2 layer on the titanium surface promoted calcification. Generally, a modified implant surface promotes the bone formation. It was reported that titanium surfaces with a nanoscale surface structure enhance proliferation and differentiation of osteoblasts to a greater degree than mechanically polished surfaces and microscale surface structure[25-28]. Furthermore, alkali-treated titanium surface promotes osteoinduction. Alkali treatment creates hydrophilicity and nanoporous structure of the TiO_2 layer. The surface promotes initial cell adhesion and nutrient supplying, and is advantageous for bone formation at early stages[29,30]. For the reasons, the alkali-treated membrane achieved sufficient bone formation in the critical-sized bone defect. These results agreed with the BTA and BMC measurements. The BTA of the without-membrane group was lower than that of the alkali and control groups. Owing to the lack of membrane, the without-membrane group showed insufficient osteoconduction for bone formation, in contrast with the groups with membranes. Among the groups with membrane, the alkali group showed higher BTA and BMC in the central

area than the control group. In the alkali group, the TiO_2 layer on the surface may have promoted more bone formation than observed in control group.

These results suggest that such a bioactive surface on a thin titanium membrane might be expected to yield bone regeneration around defects in the placed implant when applying the GBR with membrane technique.

CONCLUSION

Alkali-treated titanium membranes exhibited a high apatite-forming ability in a body-simulating environment and high bone forming ability. These results suggest that a bioactive titanium membrane can promote bone regeneration for GBR.

ACKNOWLEDGMENTS

This study was supported by the Scientific Research Grant (No. 18K09683 and 18K17122) from the Japan Society for the Promotion of Science.

CONFLICT OF INTEREST

The authors declare no competing financial interests.

REFERENCES

1) Degidi M, Scarano A, Piattelli A. Regeneration of the alveolar crest using titanium micromesh with autologous bone and a resorbable membrane. J Oral Implantol 2003; 29: 86-90.
2) Her S, Kang T, Fien MJ. Titanium mesh as an alternative to a membrane for ridge augmentation. J Oral Maxillofac Surg 2012; 70: 803-810.
3) Rakhmatia YD, Ayukawa Y, Furuhashi A, Koyano K. Current barrier membranes: titanium mesh and other membranes for guided bone regeneration in dental applications. J Prosthodont Res 2013; 57: 3-14.
4) Cole BJ, Bostrom MP, Pritchard TL, Sumner DR, Tomin E, Lane JM, *et al.* Use of bone morphogenetic protein 2 on ectopic porous coated implants in the rat. Clin Orthop Relat Res 1997; 345: 219-228.
5) Ferretti C, Ripamonti U. Human segmental mandibular defects treated with naturally derived bone morphogenetic proteins. J Craniofac Surg 2002; 13: 434-444.
6) Ban S, Iwaya Y, Kono H, Sato H. Surface modification of titanium by etching in concentrated sulfuric acid. Dent Mater 2006; 22: 1115-1120.
7) Hamouda IM, Enan ET, Al-Wakeel EE, Yousef MK. Alkali and heat treatment of titanium implant material for bioactivity. Int J Oral Maxillofac Implants 2012; 27: 776-784.
8) Iwaya Y, Machigashira M, Kanbara K, Miyamoto M, Noguchi K, Izumi Y, *et al.* Surface properties and biocompatibility of acid-etched titanium. Dent Mater J 2008; 27: 415-421.
9) Jemat A, Ghazali MJ, Razali M, Otsuka Y. Surface modifications and their effects on titanium dental implants. Biomed Res Int 2015; 2015: 791725.
10) Le Guéhennec L, Soueidan A, Layrolle P, Amouriq Y. Surface treatments of titanium dental implants for rapid osseointegration. Dent Mater 2007; 23: 844-854.
11) Offermanns V, Andersen OZ, Riede G, Sillassen M, Jeppesen CS, Almtoft KP, *et al.* Effect of strontium surface-functionalized implants on early and late osseointegration: A histological, spectrometric and tomographic evaluation. Acta Biomater 2018; 69: 385-394.
12) Shi X, Nakagawa M, Kawachi G, Xu L, Ishikawa K. Surface modification of titanium by hydrothermal treatment in Mg-containing solution and early osteoblast responses. J Mater Sci Mater Med 2012; 23: 1281-1290.
13) Kokubo T, Miyaji F, Kim HM. Spontaneous formation of bone like apatite layer on chemically treated titanium metals. J Am Ceram Soc 1996; 79: 1127-1129.
14) Kono H, Miyamoto M, Ban S. Bioactive apatite coating on titanium using an alternate soaking process. Dent Mater J 2007; 26: 186-193.
15) Kawai T, Takemoto M, Fujibayashi S, Akiyama H, Tanaka M, Yamaguchi S, *et al.* Osteoinduction on acid and heat treated porous Ti metal samples in canine muscle. PLoS One 2014; 9: e88366.
16) Umehara H, Kobatake R, Doi K, Oki Y, Makihara Y, Kubo T, *et al.* Histological and bone morphometric evaluation of osseointegration aspects by alkali hydrothermally treated implants. Appl Sci 2018; 8: 635.
17) Kobatake R, Doi K, Oki Y, Umehara H, Kawano H, Kubo T, *et al.* Investigation of effective modification treatments for titanium membranes. Appl Sci 2017; 10: 1022.
18) Camargo WA, Takemoto S, Hoekstra JW, Leeuwenburgh SCG, Jansen JA, van den Beucken JJJP, *et al.* Effect of surface alkali-based treatment of titanium implants on ability to promote in vitro mineralization and in vivo bone formation. Acta Biomater 2017; 15: 511-523.
19) Nishiguchi S, Fujibayashi S, Kim HM, Kokubo T, Nakamura T. Biology of alkali- and heat-treated titanium implants. J Biomed Mater Res A 2003; 67: 26-35.
20) Nishiguchi S, Kato H, Neo M, Oka M, Kim HM, Kokubo T, *et al.* Alkali- and heat-treated porous titanium for orthopedic implants. J Biomed Mater Res 2001; 54: 198-208.
21) Hatakeyama W, Taira M, Ikeda K, Sato H, Kihira H, Takemoto S, *et al.* Bone regeneration of rat critical-size calvarial defects using a collagen/porous-apatite composite: micro-CT analyses and histological observations. J Oral Tissue Engin 2017; 15: 49-60.
22) Andrukhov O, Huber R, Shi B, Berner S, Rausch-Fan X, Moritz A, *et al.* Proliferation, behavior, and differentiation of osteoblasts on surfaces of different microroughness. Dent Mater 2016; 32: 1374-1384.
23) Kim HM, Himeno T, Kawashita M, Lee JH, Kokubo T, Nakamura T. Surface potential change in bioactive titanium metal during the process of apatite formation in simulated body fluid. J Biomed Mater Res A 2003; 67: 1305-1309.
24) Kokubo T, Pattanayak DK, Yamaguchi S, Takadama H, Matsushita T, Kawai T, *et al.* Positively charged bioactive Ti metal prepared by simple chemical and heat treatments. J R Soc Interface 2010; 7: 503-513.
25) de Oliveira PT, Zalzal SF, Beloti MM, Rosa AL, Nanci A. Enhancement of *in vitro* osteogenesis on titanium by chemically produced nanotopography. J Biomed Mater Res A 2007; 80: 554-564.
26) Yao C, Slamovich EB, Webster TJ. Enhanced osteoblast functions on anodized titanium with nanotube-like structures. J Biomed Mater Res A 2008; 85: 157-166.
27) Goldman M, Juodzbalys G, Vilkinis V. Titanium surfaces with nanostructures influence on osteoblasts proliferation: A systematic review. J Oral Maxillofac Res 2014; 5: e1.
28) Karazisis D, Petronis S, Agheli H, Emanuelsson L, Norlindh B, Johansson A, *et al.* The influence of controlled surface nanotopography on the early biological events of osseointegration. Acta Biomater 2017; 15: 559-571.
29) Mendonça G, Mendonça DB, Aragão FJ, Cooper LF. Advancing dental implant surface technology-From micron- to nanotopography. Biomaterials 2008; 29: 3822-3235.
30) Dalby MJ, McCloy D, Robertson M, Wilkinson CD, Oreffo RO. Osteoprogenitor response to defined topographies with nanoscale depths. Biomaterials 2006; 27: 1306-1315.